## *Response to Reviews:*

We thank the three Anonymous Reviewers for their comments on our manuscript.

---

## *Reviewer #1 Comments:*

This study presents a GPP estimate over the conterminous US using TROPOMI SIF calibrated against eddy-covariance sites, with MODIS-based downscaling to 500 m spatial resolution. The methods used here are an extension of the previous work of Turner et al. (2020). This GPP estimate is then employed to examine interannual variations in GPP between 2018 and 2019, finding that differences between years are strongly impacted by four large precipitation-driven climate anomalies. This paper is well written, and I believe that this analysis is a significant scientific contribution and will be of interest to the readership of Biogeosciences. I feel that this paper is suitable for publication after generally minor revisions.

We appreciate the reviewers comments and feedback.

### *Comments*

However, as a potential user of this datasets, I feel that the impact of this work would be significantly increased if a comparison with existing (particularly MODIS-based) GPP estimates was presented. Over the past several years, there have been a number of gridded GPP products developed, including the FLUXCOM GPP (Jung et al., 2020) and FluxSat v2 GPP (Joiner et al., 2020) that estimate GPP from MODIS data trained on eddy-covariance observations. A clear advantage of the MODIS-based GPP estimates is that they cover 2001-present, while the advantages of this TROPOMI-based GPP product are less clear. In particular, some questions that I have after reading this manuscript are: (1) Would the MODIS-based GPP estimates similarly find that 2018-2019 differences in GPP to be <4% with 28% of the variations explained by these four events? (2) Do MODIS-based GPP estimates show less IAV for forest ecosystems, as suggested by NIRv? (3) SIF and NIRv may underestimate drought-induced GPP reductions (e.g., He et al., 2020), what are the differences in drought-induced GPP reductions for TROPOMI-based and MODIS-based GPP? I encourage the authors to provide a comparison of the GPP estimated in this analysis with MODIS-based estimates.

This is an excellent suggestion from the reviewer. We now include a comparison of the FLUXCOM GPP and FluxSat GPP in addition to the comparison with NIRv and LAI.

Below is a figure showing the CONUS seasonal cycle for FLUXCOM (solid lines) and TROPOMI dashed lines. We note that TROPOMI finds a more abrupt seasonal cycle and more pronounced year-to-year differences than FLUXCOM. In response to the reviewer's question, it does seem that GPP estimates using MODIS data that are trained on eddy-covariance observations show less IAV across CONUS.

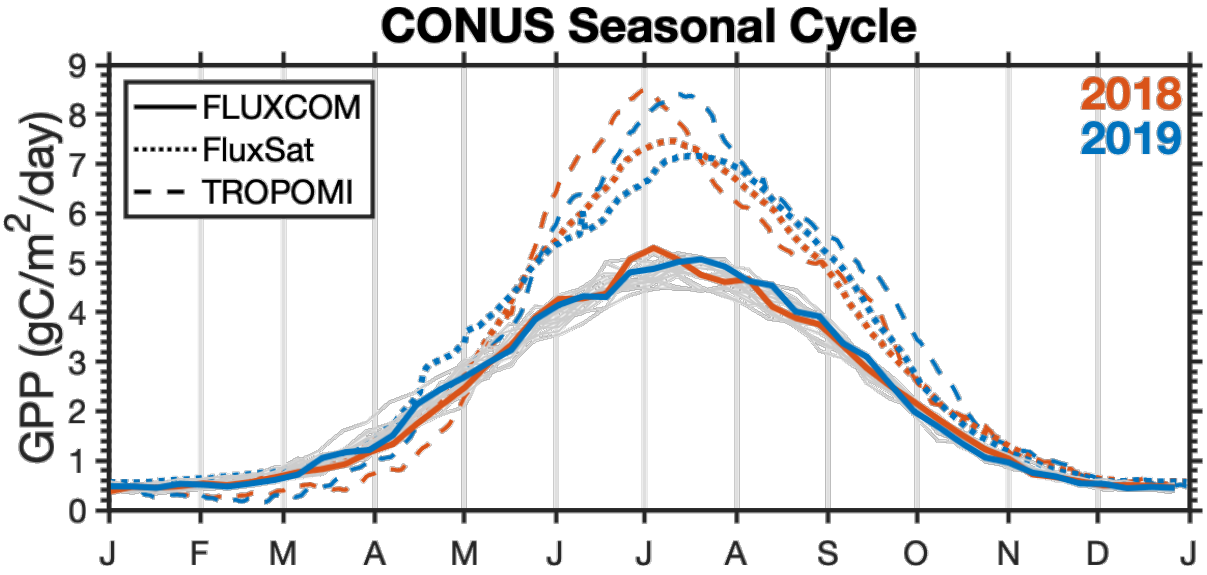


The manuscript does not provide much discussion of the uncertainties associated with these GPP estimates, and it is unclear if the GPP product provided with this analysis has associated uncertainties. I encourage the authors to include an uncertainty estimate with the data product and explain these uncertainties in the text. Presumably, an uncertainty estimate could be obtained from the uncertainty in the SIF-GPP regression.

Excellent point. We now include an uncertainty estimate by propagating the uncertainties in the SIF data and the SIF-GPP relationship:

Our estimate of GPP is proportional to SIF and the regression coefficients: $\mathrm{GPP} \propto \overline{\mathrm{SIF}} \cdot s_i$. As such, we propagate our uncertainties in quadrature:

$$\sigma_{\mathrm{GPP}} = \sqrt{\left(\frac{\partial \mathrm{GPP}}{\partial \overline{\mathrm{SIF}}}\sigma_{\overline{\mathrm{SIF}}}\right)^2 + \sum_i \left(\frac{\partial \mathrm{GPP}}{\partial s_i}\sigma_{s_i}\right)^2} \tag{7}$$

$$= \sqrt{\left(\sigma_{\overline{\mathrm{SIF}}}\gamma \sum_i s_i f_i(x,y)\right)^2 + \sum_i \left(\overline{\mathrm{SIF}}(x,y,t)\cdot \sigma_{s_i}\gamma s_i f_i(x,y)\right)^2}$$

where $\sigma_{\overline{\mathrm{SIF}}}$ is the uncertainty in the daily corrected SIF and $\sigma_{s_i}$ is the uncertainty in the SIF-GPP relationship.

## *Specific Comments*

***1)*** P2 L18-20: Please re-word this sentence. Drought and flooding are drivers of IAV but seasonal redistribution is a response.

Done.

P2 L18: *"Previous work has identified effects and responses such as drought (e.g., Sun et al., 2015), flooding (Yin et al., 2020), and seasonal redistribution (Butterfield et al., 2020) as important factors controlling interannual variability in GPP."*

***2)*** P2 L19: Check citation format. Many instances where “Author (year)” should be “(Author, year)”

We thank the reviewer for catching these issues. We have gone through all the references and corrected any LaTeX formatting issues.

***3)*** P3 L6: “partitioned by the group operating the site”. Is this always nighttime partitioning? Or does it vary between sites?

For consistency we no longer use GPP from the individual groups. We now compute GPP ourselves with nighttime partitioning at each site.

***4)*** P3 L8: It is not clear what product is being used to define the IGBP product and version number (note that there are large changes in v6 of MODIS product).

This classification is based on the land type reported with the AmeriFlux data. We have clarified this in the text.

***5)*** P4 L4: “small signal” is “small SIF signal”?

Done.

***6)*** P4 L7-16: A little bit more detail could be given in this paragraph. Are you performing the cluster analysis on the 500 m gridcells?

We downscale each TROPOMI scene to 500-m spatial resolution and then find the pixels that contain AmeriFlux sites. We then regress SIF on GPP and perform a cluster analysis on the regression slopes.

We have elaborated on this discussion in the updated manuscript:

P4 L16: *“Many of the ecosystems exhibit a similar linear relationship between SIF and GPP, which begs the question: “what ecosystems have a distinct SIF-GPP relationship?” To address this, we bootstrap the bisquare regression for each ecosystem 2000 times. The slopes from this bootstrap can be seen in Figure 2. … We then use a two component Gaussian mixture model (see, for example, Bishop 2007) to identify clusters of ecosystems with a similar SIF-GPP relationship.”*

***7)*** P4 L15: “most robust” – how is this determined?

This was assessed through repeated analysis using mixture models of different sizes. We now include a supplemental table and figure for a Gaussian Mixture Model with 3, 4, and 5 Gaussians. A “hard clustering” of the data only results in 2 Gaussians that are the dominant term for an ecosystem see Supplemental Table SXX. This is because ecosystems like

Woody Savanna and Deciduous Broadleaf have a large spread in their regression slopes. As such, there is a lot of uncertainty and the mixture model finds that those ecosystems do not require unique regression slopes.

***8)*** Figure 2: The colors for mixed forest and deciduous broadleaf are hard to distinguish and the histograms largely overlap. I suggest switching these to more contrasting colors.

The issue is that Mixed Forest has a large spread and actually lies behind the other histograms. Unfortunately, we tested a number of different color schemes and were unable to find one that drastically improve the visibility for mixed forest.

***9)*** P7 L11: "(500 mm vs 1000 mm)" – I could not find where the precipitation dataset is described. Please check that the precipitation dataset is described and cited.

We have updated the text:

P6 L26: "as inferred by measurements from the Global Precipitation Measurement (GPM) mission (specifically, we use the GPM_3IMERGDE.06 product)"

***10)*** P7 L30: "toto"

We believe this is grammatically correct. "In toto" is an adverb meaning "as a whole". This clause signifies how the various events come together to impact the total US GPP.

---

## *Reviewer #2 Comments:*

Turner and others use SIF observations to estimate GPP across the U.S. and note that its interannual variability is driven in large part by extreme events. There are many interesting elements to the manuscript, but many aspects were difficult to follow and/or incompletely described which made it difficult to be confident in the results.

We appreciate the reviewer comments and have updated the manuscript to address them.

Referencing could be improved in many places (e.g. lines 19 & 22. On p. 2. Consecutive line numbering is so helpful, please don't re-start the line numbers on every page as a courtesy to reviewers.)

Unfortunately, this is the line numbering format is defined by the Copernicus LaTeX style sheet that accompanies Biogeosciences manuscripts. As such, this is the expected format for BGD manuscripts.

### *Comments*

***1)*** Figure 1: I have questions. Some of the sites shown are meant to study lakes or are in mountainous terrain, but it is hard to tell. Is there no list of sites used? Such a table would be extremely useful in the Supplement, and also to credit the data providers for their efforts in making the data available. At least one, if not more, appears to be a NEON site (anything starting with 'x'), which is fine but NEON should be credited. Ah, I see now that the sites are listed in the Acknowledgements. This is nice but a table would be more useful to the reader. (And US-Men is meant to study a lake. A table with ecosystem type and latitude/longitude would be helpful all around.)

***2)*** Why were no eddy covariance sites in three of the four areas denoted as important for interannual variability (Texas, South Dakota, and Illinois/Indiana/Ohio) used? I understand that data are only intermittently available, but the Nebraska Mead sites may be a reasonable stand-in and the Indiana sites may be helpful.

We respond to comment #1 and #2 together as they are linked. We included all sites in the conterminous US that had data coincident with TROPOMI observations. There are many sites that did not have data available during the TROPOMI time period. TROPOMI launched in October 2017 and did not provide continuous data until 2018. We did not specifically preclude any sites. We now include a table in the supplement listing all the sites.

***3)*** How was GPP estimated? Was this consistently using the nighttime (Reichstein et al., 2005 or similar) approach? If so was it consistently with the Reichstein algorithm? This uses a unique u* threshold every few months and respiration model parameters that change as a function of time. If these are interspersed with GPP estimates that use a different approach there will be differences in seasonality of GPP estimates due to methodological differences alone.

The reviewer is correct in identifying inconsistencies in the GPP methodology. The most obvious differences were in the methodologies used by the different groups operating the AmeriFlux sites. For example, some sites enforce a lower bound of zero for GPP whereas other sites do not (they allow variability with a mean of zero).

The choice made here was to use the GPP that has been partitioned by the group operating the site (if available) as they are most familiar with their site. If the group operating the site does not provide GPP then we compute it using nighttime NEE to obtain respiration. Again, our logic for this was that the groups operating the sites know them best and we should use their reported GPP.

In response to the reviewer comments we now compute GPP ourselves for all sites using nighttime NEE to partition GPP and respiration (Reichstein et al., 2005). We have changed this methodology to avoid inconsistencies in the computation of GPP.

P3 L6: *"We compute GPP at each site using nighttime measurements of NEE as a proxy for ecosystem respiration (Reichstein et al., 2005) to partition the NEE into respiration and GPP."*

***4)*** Figure 2: I'm not entirely convinced that the 'dominant cluster' approach is useful or even necessary given that the peaks of the pdfs vary between about 15 (mixed forest) and 17 (evergreen needleleaf forest) and that estimating these land cover types using MODIS is rather well-established.

As stated in the manuscript, the question addressed by this analysis is: *"what ecosystems have a distinct SIF-GPP relationship?"* This cluster analysis across a diverse set of eddy flux sites allows us to identify unique relationships that arise between TROPOMI SIF and eddy flux GPP. This is useful because it then allows other researchers to estimate GPP from SIF even if their region does not include eddy flux towers in all ecosystems. This question was motivated by our own previous work in California (Turner et al., 2020). In that work we did not have eddy flux data in forest systems. As such, we were unable to say anything about those systems.

***5)*** In Table 1, is the value behind the +/- sign the standard error of the mean or the standard deviation? (I'm assuming its not the variance). The table legend was not described in very much detail.

The +/- is the diagonal of the covariance matrix for that Gaussian as inferred from the Gaussian Mixture Model. We now add citations with more information on GMMs:

P4 L34: *"The uncertainty is the variance for the Gaussian for that particular cluster (see Bishop, 2007; Turner and Jacob, (2015); for more on Gaussian mixture models)."*

***6)*** Per the previous comment, the structure of the manuscript was a bit bewildering. It was difficult to determine how the methodology took place because methods were interspersed throughout the manuscript starting on Page 1 with the equations. For example, I appreciate that uncertainty is (mostly) noted about carbon flux estimates but how is this uncertainty determined? Is the bootstrapping approach used to determine the uncertainty of the SIF-GPP relationship which is then propagated? Is uncertainty owing from the 16-day moving window used?

Following Reviewer #1's suggestion, we now include a paragraph discussing how we propagate uncertainty in our work:

P6 L11:

Our estimate of GPP is proportional to SIF and the regression coefficients: $\mathrm{GPP} \propto \overline{\mathrm{SIF}} \cdot s_i$. As such, we propagate our uncertainties in quadrature:

$$\sigma_{\mathrm{GPP}} = \sqrt{\left(\frac{\partial \mathrm{GPP}}{\partial \overline{\mathrm{SIF}}}\sigma_{\overline{\mathrm{SIF}}}\right)^2 + \sum_i \left(\frac{\partial \mathrm{GPP}}{\partial s_i}\sigma_{s_i}\right)^2} \tag{7}$$

$$= \sqrt{\left(\sigma_{\overline{\mathrm{SIF}}}\gamma \sum_i s_i f_i(x,y)\right)^2 + \sum_i \left(\overline{\mathrm{SIF}}(x,y,t)\cdot \sigma_{s_i}\gamma s_i f_i(x,y)\right)^2}$$

where $\sigma_{\overline{\mathrm{SIF}}}$ is the uncertainty in the daily corrected SIF and $\sigma_{s_i}$ is the uncertainty in the SIF-GPP relationship.

***7)*** Per the previous comment again, extreme events often happen quickly by definition. Is a 16-day moving window sufficient to fully describe how flooding of flack drought for example impacts ecosystems? I appreciate that the proposed precipitation mechanisms are described as 'hypothesized' and the notion that precipitation is the culprit makes great sense, but the devil might be in the details, which were not described again in sufficient detail.

Figure 4d demonstrates how our approach is sufficient for describing such events. In particular, we point the reviewer to the event that occurred on March 22, 2018. An atmospheric river delivered a large amount of precipitation to the state of California. This can be seen as the abrupt jump in the cumulative precipitation in 2018. We observe a coincident jump in our GPP estimate that is derived from TROPOMI SIF. As such, this serves as evidence that our approach is able to capture the types of phenomenon discussed here.

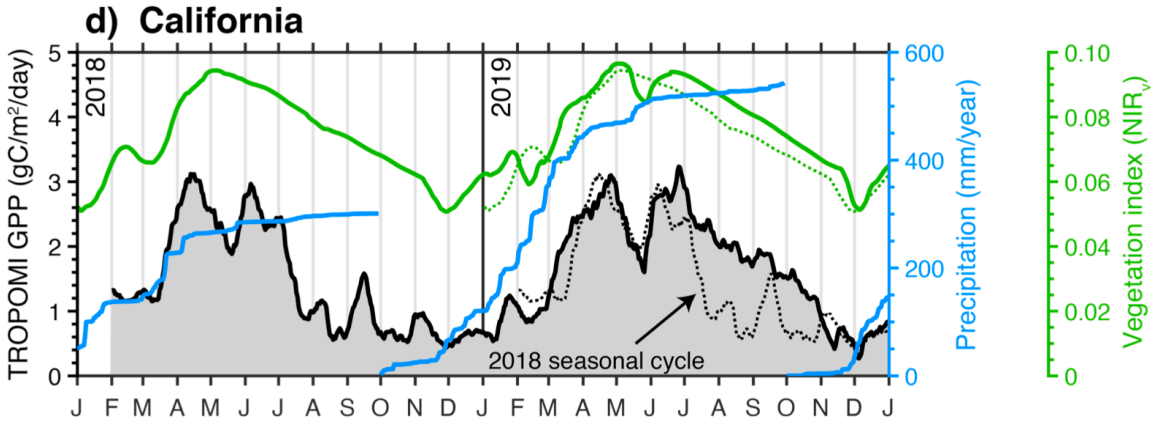


***8)*** 30: GPP does not scale linearly with PAR; the GPP/PAR relationship will usually be saturated at 1:30 pm during the growing season. How does this impact equation 4?

We have made a slight change to the way the SIF:GPP relationship is inferred that should address this. We now compute a daily corrected SIF (see, for example, Frankenberg et al., 2011; Koehler et al., 2018) that corrects for variations in overpass time, length of day, and SZA. We then compare this daily corrected SIF with the daily integrated GPP at each AmeriFlux site. The relationship is now between daily corrected SIF and daily integrated SIF. As such, we no longer need to assume linearity between GPP and PAR.

***9)*** Please note the typo in the legend of Figure 3.

Done.

---

## *Reviewer #3 Comments:*

The authors take TROPOMI SIF retrievals from 2018 and 2019 and correlate them with Ameriflux GPP estimates to calculate a relationship between SIF and GPP. They then downscale this relationship to 500m resolution using NIRV to calculate GPP over CONUS using a 16-day moving window. They find a small difference in total CONUS GPP between 2018 and 2019 (4%), and determine that 28% of this variability can be explained by 4 precipitation-associated events, in Texas, the Midwest, South Dakota, and California.

We appreciate the reviewers comments and feedback.

### *Comments*

***1.) There is nothing explicitly wrong with this paper. The methods are sound, and the results are reasonably explained by the data.*** That being said, my overall impression of the paper is that there is nothing novel or new here. The linear relationship (over large spatiotemporal scales) between SIF and GPP has been in the literature for a decade. That we can also see it in TROPOMI is not a dramatic finding. Previous work (e.g. MODSIF) has also downscaled SIF data. We also know that GPP is suppressed in drought. Again, a whole body of work. Vegetation response to drought as expressed by reduced SIF has also been previously reported. The suppression of early-season GPP due to Midwest flooding was in a paper last year. Using a new dataset to confirm previous results is not exactly groundbreaking. After reading the paper, my reaction was "well, yeah." Nothing new here, sort of a 'me too' paper, confirming previous results with a new dataset.

…

I can't in good conscience recommend a paper for publication just because they didn't do anything 'wrong'. I think there is a responsibility on the authors' part to present new, innovative and useful information to the community when submitting a paper, and I don't think that bar has been cleared here.

…

The title of the paper states that extreme events drive year-to-year variability in GPP. Between 2018 and 2019, the amount of IAV explained by the 'extreme' events emphasized is just a little over 25%. What about the other 75%? Are there other events that were not included in the study and would therefore increase the fraction of variability due to extreme events? Why were they not included? Or is the majority of IAV explained by smaller anomalies (that don't qualify as extreme) in precipitation, humidity and/or temperature? If the latter, then the paper title is demonstrably false. The claims made are qualitative, and after reading the paper I was not convinced that the title was a true statement.

…

I find myself wondering about the word 'extreme'. It's in the title (and not defined in the paper), so let's think about it a little bit. How might one define 'extreme event'? Is there a quantitative metric? I'm thinking about drought specifically, since 3 of the 4 'extreme' events involved precipitation deficit. There are multiple products that can be used to define drought (or high precipitation that might lead to flooding), such as the University of Nebraska-Lincoln Drought Monitor, Standardized Precipitation Index, or Palmer Drought Severity Index that are easily available in gridded form. It would not be difficult to define 'extreme' using one (or more) of these products and then correlate the regional differences in GPP with them. The title of the paper could then be confirmed or refuted quantitatively.

We appreciate the reviewer's positive assessment of the content and lack specific criticisms.

That said, we find the reviewer's assessment odd. While this reviewer does not seem to find the manuscript particularly interesting we contend that our manuscript is useful to the scientific community as it stands. Our manuscript presents a regional analysis of a novel dataset. We then identify the major anomalies that drive year-to-year variability in our dataset. We have also added a comparison to other independent GPP datasets (FLUXCOM and FluxSat) as well as MODIS NIRv and LAI. Further, Reviewer #1 and Reviewer #2 both specifically note that the work is interesting. As such, we argue that our work is a valuable contribution to the scientific literature and appropriately placed in a disciplinary journal such as Biogeosiences.

Regarding the Reviewer's comment *"The title of the paper states that extreme events drive year-to-year variability in GPP… Or is the majority of IAV explained by smaller anomalies (that don't qualify as extreme) in precipitation, humidity and/or temperature? If the latter, then the paper title is demonstrably false."*

We were unable to find a simple explanation (e.g., precip or humidity) for the remaining variability. Our Figure 3 shows a handful of large, obvious anomalies. Our work looked at the largest of these and found they were consistently driven by extreme precipitation events, thus the title of the paper.

***2)*** 2018-2019 differences in GPP could be stratified by drought/excess precipitation metric, and the annual difference in GPP could be quantified in terms of fractional contribution by 'extreme' (greater than +/- 1 standard deviation in the index chosen?) and fractional contribution by anomalies that don't qualify as extreme. I'd be interested to see that. One might also look at these differences on a seasonal and/or PFT-level basis. Does 'minor' (not extreme) variability in eastern CONUS drive overall CONUS variability because mean GPP is so much larger than in more arid regions (the west)? That's an interesting question as well.

We appreciate the suggestion of the reviewer and think this may be interesting to investigate in future work. However, we don't think an additional exploratory analysis is warranted for this particular manuscript.

***3)*** My formal recommendation for the paper is rejection, but I think with a little more effort the datasets the authors have produced can be used for research that has real value. If that effort can be put forth, I think resubmission would be entirely appropriate.

There were 4 main results from this paper: 1) we observe distinct relationships across different ecosystems between TROPOMI SIF and GPP, 2) we use these relationships to estimate GPP across CONUS at 500-m spatial resolution, 3) we observe small year-to-year differences in CONUS GPP (less than 4%), and 4) of the differences we do see, a large fraction of those are attributable to extreme precipitation events. All four of these results are the first of their kind.

Following suggestions from other reviewers, we have now added an additional comparison to FLUXCOM and FluxSat.

***Comments***

***1)*** Page 4, L30-31: "…by assuming that GPP scales linearly with PAR…" This statement is just plain wrong. There is a very large body of observational work that demonstrates it. The idea that the GPP/PAR relationship is nonlinear is the basis of every terrestrial biosphere model, from light-response models like VPRM or CASA to enzyme-kinetic models such as CLM, ORCHIDEE or SiB. The authors of the paper know this, so I'm assuming that there are assumptions behind this statement. They need to be explained, and the statement justified (much) more than just a statement of fact. It is not.

We have made a slight change to the way the SIF:GPP relationship is inferred that should address this. We now compute a daily corrected SIF (see, for example, Frankenberg et al., 2011; Koehler et al., 2018) that corrects for variations in overpass time, length of day, and SZA. We then compare this daily corrected SIF with the daily integrated GPP at each AmeriFlux site. The relationship is now between daily corrected SIF and daily integrated SIF. As such, we no longer need to assume linearity between GPP and PAR.

***2)*** There are multiple references that are incorrectly formatted.

Corrected.

***3)*** The annual GPP was given (0.6-0.7 PG C), but comparison to other products would be helpful. It is well-known that GPP simulations (global or regional) vary by a factor of two or more, so it would be informative to know where the GPP product generated here sits in that spectrum, not just in terms of annual total but seasonal/regional comparison as well.

We now compare to FLUXCOM and FluxSat GPP as well.

# Extreme events driving year-to-year differences in gross primary productivity across the US

Alexander J. Turner[1], Philipp Köhler[2], Troy S. Magney[3], Christian Frankenberg[2,4], Inez Fung[5], and Ronald C. Cohen[5,6]

[1]Department of Atmospheric Sciences, University of Washington, Seattle, WA, 98195, USA
[2]Division of Geological and Planetary Sciences, California Institute of Technology, Pasadena, CA, 91226, USA.
[3]Department of Plant Sciences, University of California, Davis, CA, 95616, USA.
[4]Jet Propulsion Laboratory, California Institute of Technology, Pasadena, CA, 91109, USA.
[5]Department of Earth and Planetary Sciences, University of California, Berkeley, CA, 94720, USA.
[6]College of Chemistry, University of California, Berkeley, CA, 94720, USA.

**Correspondence:** Alexander J. Turner (turneraj@uw.edu)

**Abstract.** Solar-Induced chlorophyll Fluorescence (SIF) has previously been shown to strongly correlate with gross primary productivity (GPP), however this relationship has not yet been quantified for the recently launched TROPOspheric Monitoring Instrument (TROPOMI). Here we use a Gaussian mixture model to develop a parsimonious relationship between SIF from TROPOMI and GPP from flux towers across the conterminous United States (CONUS). The mixture model indicates the SIF-GPP relationship can be characterized by a linear model with two terms. We then estimate GPP across CONUS at 500-m spatial resolution over a 16-day moving window. We ~~find that CONUS GPP varies by less than 4%between 2018 and 2019. However, we~~ observe four extreme precipitation events that induce regional GPP anomalies: drought in west Texas, flooding in the midwestern US, drought in South Dakota, and drought in California. Taken together, these events account for 28% of the year-to-year GPP differences across CONUS. Despite these large regional anomalies, we find that CONUS GPP varies by less than 4% between 2018 and 2019.

## 1 Introduction

Terrestrial gross primary productivity (GPP) is the total amount of carbon dioxide ($CO_2$) assimilated by plants through photosynthesis and represents one of the main drivers of interannual variability in the global carbon cycle Le Quéré et al. (2018). As such, quantifying the spatiotemporal patterns of terrestrial GPP is critical to understanding how the carbon cycle will both respond to and influence climate. Work over the past decade has shown satellite measurements of solar-induced chlorophyll fluorescence (SIF) to correlate strongly with tower-based estimates of GPP (e.g., Frankenberg et al., 2011a; Yang et al., 2015; Sun et al., 2017; Turner et al., 2020; Wang et al., 2020) and are often used as a remote-sensing proxy for GPP.

This relationship between SIF and GPP is typically expressed through a pair of light use efficiency models Monteith (1972) that relate GPP and SIF to the absorbed photosynthetically active radiation (APAR):

$$\mathrm{GPP} = \mathrm{APAR} \times \Phi_{\mathrm{CO_2}} \quad (1)$$

$$\mathrm{SIF} = \mathrm{APAR} \times \beta\Phi_{\mathrm{F}} \quad (2)$$

where $\Phi_{\mathrm{CO_2}}$ is the light use efficiency of $CO_2$ assimilation, $\Phi_{\mathrm{F}}$ is the fluorescence yield, and $\beta$ is the probability of fluoresced photons escaping the canopy. Solving for APAR and substituting, we can rewrite GPP as:

$$\mathrm{GPP} = \frac{\Phi_{\mathrm{CO_2}}}{\beta\Phi_{\mathrm{F}}}\mathrm{SIF}. \quad (3)$$

The derivation follows from Lee et al. (2013), Guanter et al. (2014), Sun et al. (2017), and others.

This seemingly straightforward relationship between SIF and GPP has been widely used to infer GPP from measurements of SIF (e.g., Frankenberg et al., 2011a; Parazoo et al., 2014; Yang et al., 2015, 2017; Sun et al., 2017, 2018; Magney et al., 2019; Turner et al., 2020) with some work showing that SIF captures more variability in GPP than APAR alone (e.g., Yang et al., 2015, 2017; Magney et al., 2019). However, there is much complexity encapsulated in the first term of Eq. 3 ($\Phi_{\mathrm{CO_2}}/\beta\Phi_{\mathrm{F}}$). There is an ongoing debate about what *exactly* SIF is telling us about GPP (e.g., Joiner and Yoshida, 2020; Maguire et al., 2020; Dechant et al., 2020; He et al., 2020; Marrs et al., 2020) and the spatio-temporal scales at which SIF and GPP correlate well. A recent paper from Magney et al. (2020) presents a concise summary of the covariation between SIF and GPP at different spatio-temporal scales and how non-linear relationships at the leaf-scale often integrate to a linear response at the canopy-scale. This is due, in large part, to the fact that most of our satellite measurements occur near the middle of the day when the $\Phi_{\mathrm{CO_2}}$-$\Phi_{\mathrm{F}}$ response is more-or-less linear and the observed signal is integrated over many leaves.

Here we focus on the ecosystem-scale relationship between SIF and GPP, as that is the relevant observable scale from space-borne instruments. We begin by characterizing the relationship between instantaneous SIF from TROPOMI and half-hourly GPP from flux towers. Following this, we use this ecosystem-scale relationship to infer GPP at a spatial resolution of 500-m using TROPOMI SIF measurements and identify drivers of interannual variability in GPP. Previous work has identified effects ~~such as seasonal redistribution Butterfield et al. (2020),~~ and responses such as drought (e.g., Sun et al., 2015), ~~and flooding Yin et al. (2020) as important drivers of~~ flooding (Yin et al., 2020), and seasonal redistribution (Butterfield et al., 2020) as important factors controlling interannual variability in GPP.

## 2 Identifying distinct relationships between SIF and GPP

We build on our previous work ~~Turner et al. (2020)~~ (Turner et al., 2020) downscaling measurements of SIF to 500-m spatial resolution. Briefly, the TROPOspheric Monitoring Instrument (TROPOMI; Veefkind et al., 2012) is a nadir-viewing imaging spectrometer. TROPOMI has a 2,600 km swath with a nadir spatial resolution of 5.6 km along track and 3.5 km across track. Köhler et al. (2018) presented the first retrievals of SIF from TROPOMI. As in Turner et al. (2020), we apply a *post hoc* bias correction to ensure positivity of monthly average values as systematically negative SIF values are non-physical. We downscale

individual TROPOMI scenes using the near-infrared reflectance of vegetation index ($NIR_V$) that was proposed by Badgley et al. (2017, 2019). We use the MCD43A4.006 (v06) MODIS NBAR reflectances Schaaf et al. (2002) to compute $NIR_V$. Two notable differences from Turner et al. (2020) are: 1) the analysis is extended to cover all of CONUS and 2) we now use a 16-day moving window, thus including a full orbit cycle in each averaging window to minimize effects due to viewing-illumination geometry and noise. Supplemental Fig. S3 shows the improvement when averaging to longer temporal windows with an $r$ of 0.66, 0.74, 0.79, and 0.82 for instantaneous, 8-day, 16-day, and 32-day temporal windows, respectively.

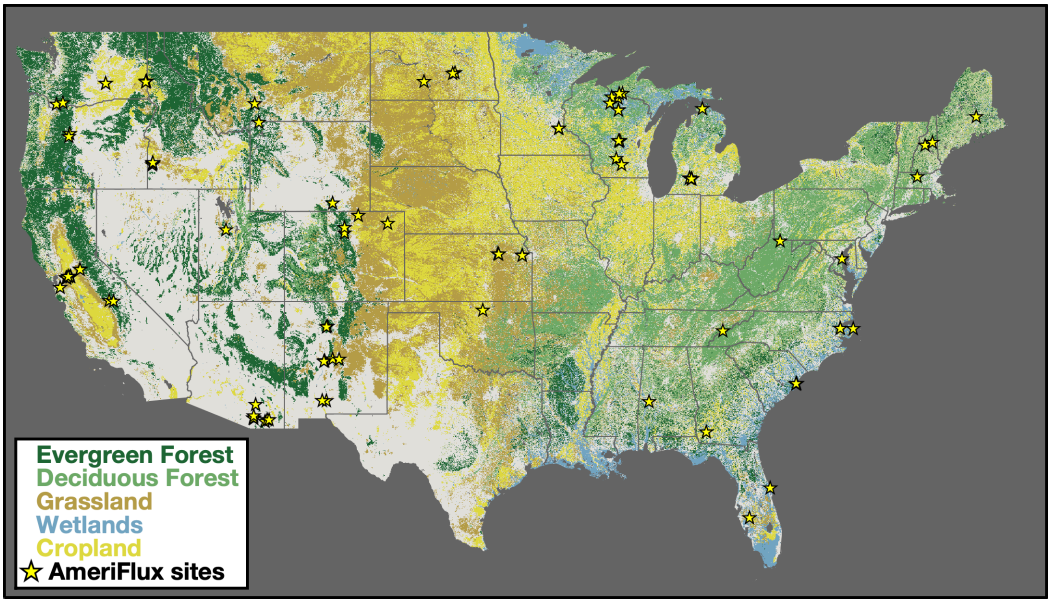


**Figure 1. Dominant landcover over conterminous United States (CONUS).** Colors show the dominant landcover over CONUS. Classification is based on the 2019 USDA CropScape database USDA (2018). Forests are shown in green croplands in yellow, and wetlands in blue. Location of 82 AmeriFlux sites used in this study are shown as yellow stars.

The extension to CONUS facilitates comparison of TROPOMI SIF retrievals to flux tower data over a more representative set of ecosystems and robustly infer the SIF-GPP relationship. Specifically, there are 82 AmeriFlux sites Baldocchi et al. (2001) within CONUS that reported data in 2018, 2019, or 2020 whereas Turner et al. (2020) only included 11 sites and did not have data from forests. Figure 1 shows the location of these 82 AmeriFlux sites overlaid on the dominant landcover. These eddy covariance sites provide a direct measure of net ecosystem exchange (NEE; $CO_2$ fluxes) Baldocchi et al. (1988). We ~~use GPP that has been partitioned by the group operating the site . If GPP is not provided we compute it~~ compute GPP at each site using nighttime measurements of NEE as a proxy for ecosystem respiration Reichstein et al. (2005) to partition the NEE into respiration and GPP. The AmeriFlux sites used here cover 10 ecosystems as defined by the International Geosphere-Biosphere Programme: evergreen needleleaf forest, deciduous broadleaf forest, mixed forest, grassland, cropland, wetland, woody savanna, savanna, open shrubland, and closed shrubland. These are the classifications reported with the AmeriFlux data as of July 2021 (https://ameriflux.lbl.gov).

We characterize the relationship between TROPOMI SIF and AmeriFlux GPP by plotting downscaled ~~instantaneous~~ SIF observations against daily GPP from the nearest AmeriFlux ~~GPP data in time~~ site (see Supplemental Figs. S1-S3). The TROPOMI overpass time varies over the orbit cycle. Frankenberg et al. (2011b) presented a simple approach to compute a "daily corrected" SIF that accounts for variations in overpass time, length of day, and solar zenith angle:

$$\overline{\mathrm{SIF}}(x,y,t) = \mathrm{SIF}(x,y,\tau_s)\frac{\int_{\tau_0}^{\tau_f}\cos\left[\mathrm{SZA}(x,y,\tau)\right]\mathrm{d}\tau}{\cos\left[\mathrm{SZA}(x,y,\tau_s)\right]} \tag{4}$$

where $\mathrm{SIF}(x,y,\tau_s)$ is the instantaneous SIF, SZA is the local solar zenith angle, $\tau_0$ is sunrise, $\tau_f$ is sunset, and $\tau_s$ is the hour corresponding to the TROPOMI overpass time. We compare this daily corrected SIF against the daily GPP for each AmeriFlux site. Specifically, the ~~6~~ 7 steps we take here are: 1) construct a timeseries of daily GPP from each AmeriFlux site, 2) apply the *post hoc* bias correction to the TROPOMI SIF data, ~~2) find all TROPOMI scenes that cover an AmeriFlux site,~~ ~~3~~3) compute the daily correction for TROPOMI SIF data, 4) downscale TROPOMI scenes to 500-m spatial resolution using MODIS $\mathrm{NIR_V}$, ~~4)~~ 5) find all TROPOMI scenes that cover an AmeriFlux site, 6) construct a timeseries of SIF observations from the 500-m grid cell that contains the AmeriFlux site, ~~5) construct a timeseries of AmeriFlux GPP data that are coincident in time with the TROPOMI overpass, and 6) regress SIF on~~ and 7) regress coincident daily corrected TROPOMI SIF on daily AmeriFlux GPP with a bisquare regression. The bisquare regression was chosen due to robustness against outliers. Additionally, we force the regression through the origin based on the physical constraint that GPP should be zero if SIF is zero. We observe a linear relationship between SIF and GPP when plotted against all ecosystems (Supplemental Figure S1) and when separated by ecosystem (Supplemental Figure S2). Notable exceptions are closed shrubland, open shrubland, and savanna ecosystems where SIF explains less than 10% of the variability in GPP for AmeriFlux sites in those ecosystems due, in part, to a low signal-to-noise ratio. These ecosystems typically have a small SIF signal and the bright surfaces often result in a higher retrieval uncertainty. This combination of a small signal and high retrieval uncertainty results in a low signal-to-noise ratio, complicating efforts to derive a robust relationship between SIF and GPP for these ecosystems.

Many of the ecosystems exhibit a similar linear relationship between SIF and GPP, which begs the question: *"what ecosystems have a distinct SIF-GPP relationship?"* To address this, we bootstrap the bisquare regression for each ecosystem 2000 times. The slopes from this bootstrap can be seen in Figure 2. The range of slopes vary from 13 to 18 $\left(\mu\mathrm{mol\,m^{-2}\,s^{-1}}\right)/\left(\mathrm{mW\,m^{-2}\,sr^{-1}\,s^{-1}}\right)$ with grasslands at the low end and evergreen needleleaf forests at the high end. We then use a two component Gaussian mixture model (see, for example, Bishop, 2007) to identify clusters of ecosystems with a similar SIF-GPP relationship. The implementation of our Gaussian mixture model is adapted from Turner and Jacob (2015). Parameters of the mixture model are obtained via an iterative expectation-maximization algorithm. A drawback of these mixture models is they often find local minima. To address this, we repeat the fitting of the mixture model with multiple initializations and use simulated annealing to search for a global minimum. We tested a range of mixture model sizes and found a mixture of two Gaussians to be the most robust. Adding additional terms in the model resulted in Gaussians that did not have the largest weighting factor for any ecosystem. This is because ecosystems like Woody Savanna and Deciduous Broadleaf have a large spread in their slope. As such, there

is a lot of uncertainty and the model does not find that they require a unique regression slope. The resulting mixture model is overlaid on the histogram in Figure 2.

We observe a clustering of ecosystems with SIF-GPP relationships around 16.4 $\left(\mu\mathrm{mol\,m^{-2}\,s^{-1}}\right) / \left(\mathrm{mW\,m^{-2}\,sr^{-1}\,s^{-1}}\right)$. This grouping is the dominant weighting term for wetlands, evergreen needleleaf forest, deciduous broadleaf forest, mixed forest, cropland, and woody savanna. We refer to this cluster as the "Dominant Cluster" and assume that ecosystems not specifically mentioned elsewhere will have a response that is similar to this primary cluster. The other component of the mixture model corresponds to grasslands. Ecosystems not explicitly mentioned use the "Dominant Cluster" for scaling SIF to GPP. Table 1 lists the SIF-GPP relationships for these two clusters. The uncertainty is the variance for the Gaussian for that particular cluster (see Bishop, 2007; Turner and Jacob, 2015, for more on Gaussian mixture models). Previous work has also found unique SIF-GPP relationships between C3 and C4 plants using measurements from a tower including a non-linear response in C3 plants ~~He et al. (2020)~~(He et al., 2020), we examined this here using two AmeriFlux sites in corn fields and two in potato fields. We do observe potential differences in the SIF-GPP relationship between these C3 and C4 systems (see Supplemental Figure S5). The difference in SIF-GPP relationship for C3 and C4 systems seen here is also similar to what was observed using $\mathrm{NIR_v}$ Badgley et al. (2019). These relationships can be used to reconstruct GPP from TROPOMI SIF as: $\mathrm{GPP} = \mathrm{SIF} \times \left(\sum_i f_i s_i\right)$ where $s_i$ is the SIF-GPP relationship in Table 1 for the $i^{\mathrm{th}}$ cluster and $f_i$ is the fraction of a grid cell represented by that cluster.

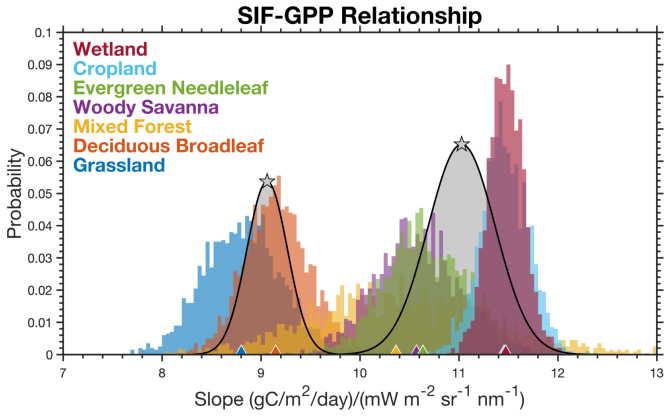


**Figure 2. Identifying distinct SIF-GPP relationships across ecosystems.** Histogram shows the distribution of slopes that map SIF to GPP using a bisquare regression and a 2000 member bootstrap. Colors denote the different ecosystems and triangles at the bottom show the mean for that ecosystem. Gray distributions are from a two-member Gaussian Mixture Model and the stars indicate the mean for that component.

TROPOMI is in low earth orbit and only observes a snapshot in time. The equatorial overpass time at nadir is 13:30 local time. ~~By assuming that GPP scales linearly with PAR (i.e., Eq. 1) we can compute a correction factor to estimate daily integrated GPP.~~ We compute a daily corrected SIF that accounts for variations in overpass time, length of day, and solar zenith

**Table 1.** SIF-GPP relationships for different groupings.

| Cluster | SIF-GPP relationship[a] ($s_i$) |
|---|---|
| Dominant Cluster | ~~16.4~~ 9.1 ± ~~0.4~~ 0.2 |
| Grassland | ~~14.1~~ 11.0 ± ~~0.1~~ 0.3 |

[a]All SIF-GPP relationships have units of $\left(\mathrm{gC\ m^{-2}\ day^{-1}}\right) / \left(\mathrm{mW\ m^{-2}\ sr^{-1}\ nm^{-1}}\right)$. Uncertainty is the diagonal of the covariance matrix for the mixture model.

angle (Frankenberg et al., 2011b; Köhler et al., 2018):

$$\overline{\mathrm{SIF}}(x,y,t) = \mathrm{SIF}(x,y,\tau_s)\frac{\int_{\tau_0}^{\tau_f}\cos\left[\mathrm{SZA}(x,y,\tau)\right]\mathrm{d}\tau}{\cos\left[\mathrm{SZA}(x,y,\tau_s)\right]} \tag{5}$$

where $\mathrm{SIF}(x,y,\tau_s)$ is the instantaneous SIF, SZA is the local solar zenith angle, $\tau_0$ is sunrise, $\tau_f$ is sunset, and $\tau_s$ is the hour corresponding to the TROPOMI overpass time. We use this daily corrected SIF in conjunction with More formally, we scale the instantaneous SIF by the ratio of the integral of the cosine of the solar zenith angle (SZA) over the day to $\cos(\mathrm{SZA})$ from the TROPOMI overpass time. Putting everything together, we estimate daily GPP from TROPOMI SIF observations as:

$$\mathrm{GPP}(x,y,t) = \mathrm{SIF}\overline{\mathrm{SIF}}(x,y,t)\cdot\gamma\sum_i s_i f_i(x,y)\cdot\frac{\int_{\tau_0}^{\tau_f}\cos\left[\mathrm{SZA}(x,y,\tau)\right]\mathrm{d}\tau}{\cos\left[\mathrm{SZA}(x,y,\tau_s)\right]} \tag{6}$$

where $\mathrm{SIF}(x,y,t)$ is the 500-m downscaled SIF using a 16-day moving window, $\gamma$ is a unit conversion from $\mu$mol to gC, $s_i$ is the SIF-GPP relationship inferred from comparison with AmeriFlux GPP (see Table 1), $f_i(x,y)$ is the fraction of the grid cell represented by the $i^{\mathrm{th}}$ cluster, SZA is the local solar zenith angle, $\tau_0$ is sunrise, $\tau_f$ is sunset, and $\tau_s$ is the hour corresponding to the TROPOMI overpass time. We do not include information on cloud cover in our approach, this could potentially be included in the future to account for diurnal variations in PAR.

Our estimate of GPP is proportional to SIF and the regression coefficients: $\mathrm{GPP} \propto \overline{\mathrm{SIF}}\cdot s_i$. As such, we propagate our uncertainties in quadrature:

$$\begin{aligned}\sigma_{\mathrm{GPP}} &= \sqrt{\left(\frac{\partial\mathrm{GPP}}{\partial\overline{\mathrm{SIF}}}\sigma_{\overline{\mathrm{SIF}}}\right)^2 + \sum_i\left(\frac{\partial\mathrm{GPP}}{\partial s_i}\sigma_{s_i}\right)^2} \\ &= \sqrt{\left(\sigma_{\overline{\mathrm{SIF}}}\gamma\sum_i s_i f_i(x,y)\right)^2 + \sum_i\left(\overline{\mathrm{SIF}}(x,y,t)\cdot\sigma_{s_i}\gamma s_i f_i(x,y)\right)^2}\end{aligned} \tag{7}$$

where $\sigma_{\overline{\mathrm{SIF}}}$ is the uncertainty in the daily corrected SIF and $\sigma_{s_i}$ is the uncertainty in the SIF-GPP relationship.

## 3 Drivers of interannual variations in US gross primary productivity

Figure 3 shows annual mean GPP across CONUS inferred from TROPOMI SIF measurements using Eq. 6. A number of prominent features are visible such as the Central Valley of California, the Snake River Valley in Idaho, and the Adirondack Mountains in upstate New York. California's Central Valley and Idaho's Snake River Valley are both major agricultural regions in the western US (e.g., the Central Valley of Califoria accounts for more than 15% of irrigated land in the US). The Adirondack Mountains are a roughly circular dome that rise above the surrounding lowlands, resulting in a shorter growing season and lower annual mean GPP. This shortened growing season can be seen in an animation of GPP over CONUS (Supplemental Movie S1).

We observe substantial GPP across the eastern US (delineated here by 98°W) with annual mean values generally in excess of 5 gC/m$^2$/day. This region accounts for less than half of the land but more than 70% of the annual GPP. This delineation in GPP roughly coincides with the location of drylands in CONUS that are more sensitive to changes in precipitation as inferred by measurements from the Global Precipitation Measurement (GPM) mission (specifically, we use the GPM_3IMERGDE.06 product); drylands are also projected to expand in future climate Yao et al. (2020). Most of the large year-to-year differences occur in these western US drylands (see Fig. 3c), a notable exception being a negative GPP anomaly in 2019 relative to 2018 that extended across Illinois, Indiana, and Ohio. Here we highlight four precipitation-driven GPP anomalies, which taken together, account for 28% of the interannual GPP variability across the United States: 1) 2018 drought in west Texas, 2) 2019 midwestern crop flooding, 3) 2018 drought in South Dakota, and 4) 2018 drought in California. Figure 4 summarizes the interannual precipitation differences that we hypothesize are responsible for explaining these four GPP anomalies.

The largest positive GPP anomaly in 2019 relative to 2018 was observed across western Texas. This single event accounted for 11% of the year-to-year difference in GPP across CONUS with an annual GPP of 0.65 $\pm$ 0.47 PgC in 2018 and 0.76 $\pm$ 0.45 PgC in 2019. From Figure 4a, we observe 50% higher GPP in spring 2019 compared to spring 2018. This increase in GPP was driven by a lack of precipitation in spring 2018. The cumulative precipitation from October 2017 through June 2018 was 50% less than October 2018 through June 2019 (500 mm vs 1000 mm). The other notable difference between GPP in 2018 and 2019 was a second peak during fall 2018 that was not present in 2019. This second peak coincided with a series of precipitation events beginning in early September. This tight coupling between GPP and precipitation is expected for dryland systems such as west Texas (e.g., Smith et al., 2019). The seasonal GPP dynamics inferred from TROPOMI SIF are also present in the MODIS vegetation index NIR$_\mathrm{v}$, albeit with slight differences in magnitude, implying convergent responses in SIF and NIR$_\mathrm{v}$ for this ecosystem.

The second largest anomaly is the reduction in 2019 GPP relative to 2018 across midwestern crop areas (specifically Illinois, Indiana, and Ohio) that accounted for 7% of the year-to-year difference in CONUS GPP. The 2018 annual GPP was 0.70 $\pm$ 0.12 PgC and 0.63 $\pm$ 0.14 PgC in 2019. We observe a decrease in the maximum GPP between 2019 and 2018 as well as a two week delay in the timing of the maximum. This anomaly was highlighted in recent work from Yin et al. (2020) who attribute the anomaly to flooding in the midwestern US. The flooding delayed planting of crops by two weeks and resulted in decreased carbon uptake across the midwestern crop areas and Mississippi Alluvial Valley, where we also observe a negative anomaly in Figure 3c. Yin et al. (2020) provide a detailed discussion of these floods and their impacts on crop productivity.

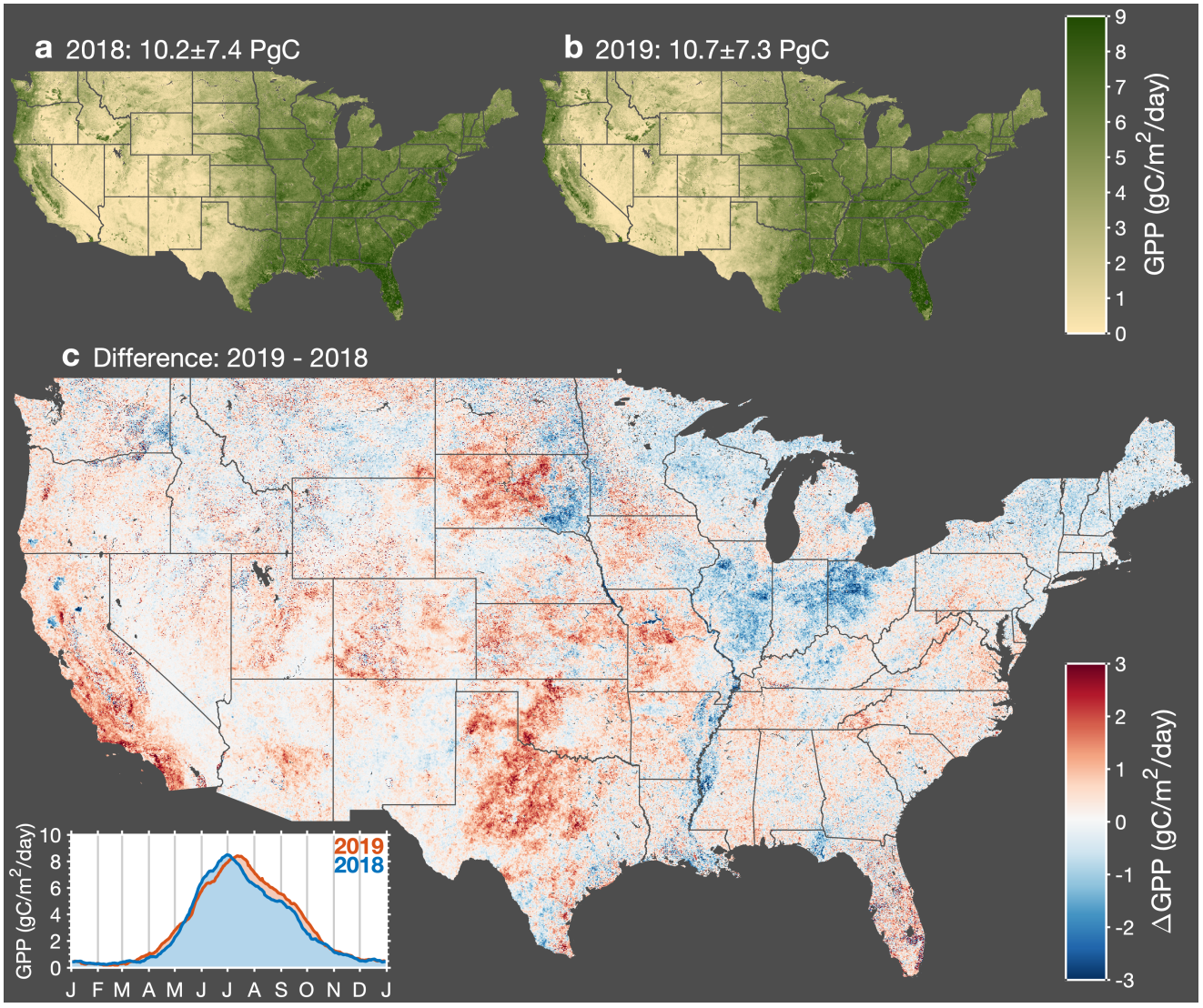


**Figure 3. Interannual variations in gross primary productivity across CONUS.** Map of annual mean GPP for 2018 (panel a) and 2019 (panel b). (Panel c) Map of the difference in annual mean GPP between 2019 and 2018. Red indicates higher GPP in 2019 and red indicates higher GPP in 2018. Inset in bottom left corner shows a timeseries of the average GPP across CONUS for 2018 and 2019.

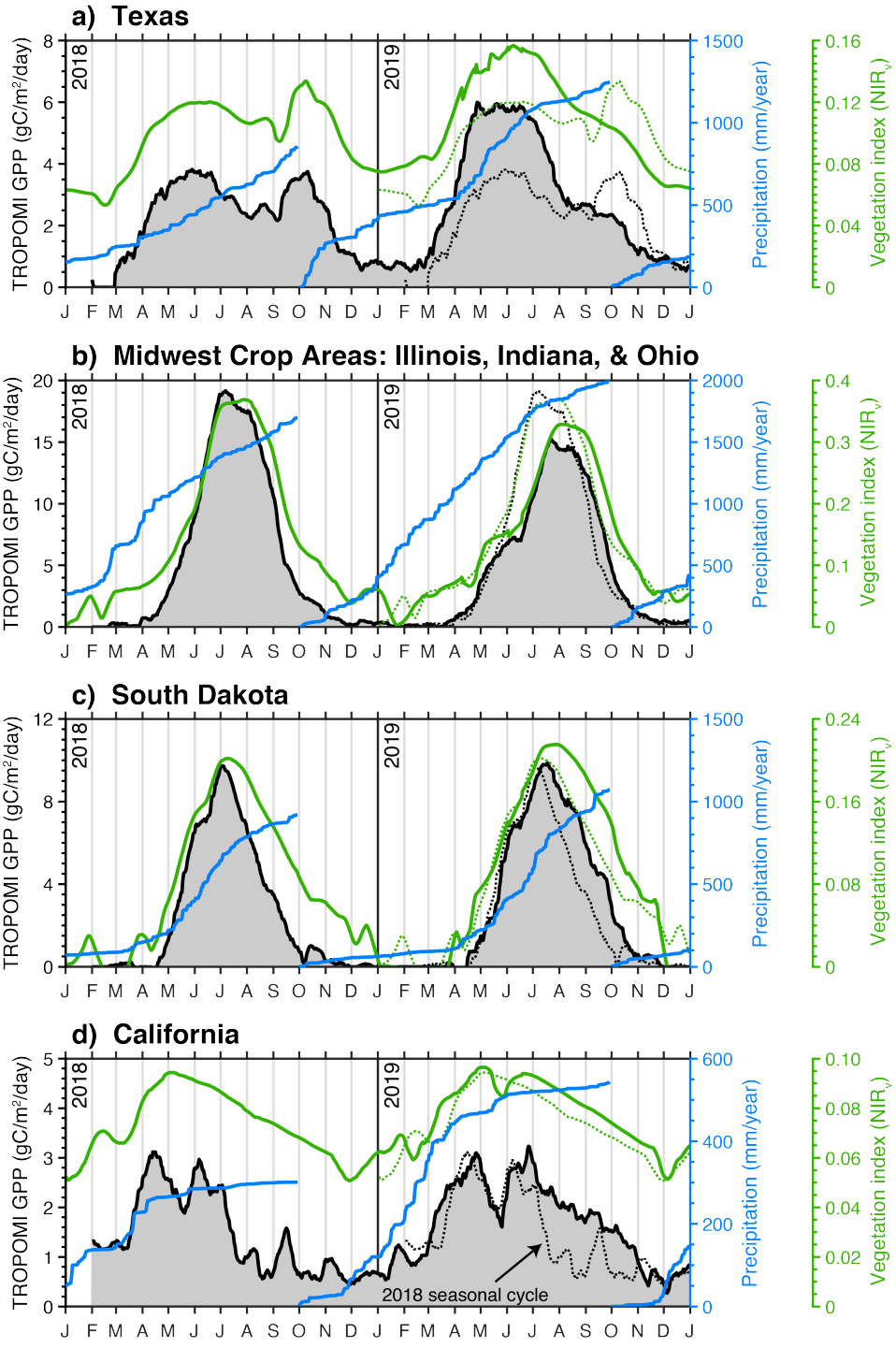


**Figure 4. Major drivers of interannual variability in CONUS GPP.** Black line shows the TROPOMI-derived GPP over Texas (a), the midwest crop region (b), South Dakota (c), and California (d). Blue line shows the cumulative precipitation over the water year as measured by the GPM satellite. Green line is $NIR_v$ from MODIS. Black and Green dotted lines are 2018 GPP and $NIR_v$ superimposed on the 2019 timeseries.

South Dakota exhibits a dipole with positive anomalies in 2019 in the west and negative anomalies in the east, again relative to 2018. The 2018 annual GPP was 0.20 $\pm$ 0.09 PgC and 0.63 $\pm$ 0.08 PgC in 2019. The negative anomalies in the east are driven by the flooding events discussed above and in Yin et al. (2020). However, the positive anomaly in western portion of the state is the dominant term. This positive anomaly is driven by a series of summer precipitation events that served to extend the growing season across the western plains. From Figure 4c, we can see three precipitation events throughout the mid-to-late summer that coincide with pauses in senesence: mid-July, early August, and mid-September. As with Texas, this highlights the tight coupling between GPP and precipitation for dryland systems. In toto, these precipitation events served to increase statewide GPP in 2019 relative to 2018.

The final notable anomaly is California's positive GPP anomaly in 2019. The 2018 annual GPP was 0.27 $\pm$ 0.24 PgC and 0.33 $\pm$ 0.26 PgC in 2019. 2018 was a mild drought in California with $\sim$80% of the state being classified as abnormally dry; 2019 had 50% more precipitation during the water year than 2018 (Figure 4c). Two consequences of this drought in 2018 were: a delayed onset of photosynthesis and a mid-summer senescence. The onset of photosynthesis in 2018 coincided with a series of atmospheric rivers that delivered about a third of the total precipitation that year, indicating a water limitation up to that point. In contrast, 2019 had ample precipitation through the winter and we observe both an earlier onset of photosynthesis and an extension of the growing season into the fall. Evergreen forests are the main contributor to the SIF signal during the summer and fall Turner et al. (2020) and, as such, will be more sensitive to the accumulated precipitation. The spatial pattern of the differences in August-November GPP (Fig. S4) strongly correlate with evergreen forests.

In contrast to the anomalies presented earlier, the SIF-derived GPP and MODIS-based vegetation index ($NIR_V$) show divergent seasonal dynamics for California. $NIR_V$ shows small differences between 2018 and 2019 with a strong similarity to the 2019 SIF-derived GPP. The seasonality of $NIR_V$ is similar to that of the leaf area index (LAI) derived from MODIS (see Supplemental Figure 6), implying a biophysical signal. Vegetation indices derived from the red and NIR part of the spectrum estimate *photosynthetic capacity* provided optimal soil moisture, temperature, and PAR are known Sellers (1985). As such, this suggests that we observed a down-regulation of photosynthesis from evergreen forests in response to a water limitation during fall 2018, whereas these forests were close to photosynthetic capacity in fall 2019 resulting in a similar seasonality to 2018 and 2019 $NIR_V$. Sims et al. (2014) also report a low sensitivity of MODIS vegetation indices to drought stress in forests.

We additionally compare our GPP estimated from TROPOMI SIF to previous work developing gridded GPP products using machine learning. Specifically, the FLUXCOM initiative (http://www.fluxcom.org/; Jung et al., 2020) and FluxSat (Joiner and Yoshida, 20 trained machine learning models to predict gridded-GPP from eddy covariance sites using remote sensing data (including MODIS). Figure 5 shows the CONUS seasonal cycle from both FLUXCOM, FluxSat, and TROPOMI. The seasonal cycles of GPP inferred from TROPOMI and FluxSat are generally in agreement with a similar magnitude while FLUXCOM predicts 35% less GPP. Additionally, the interannual variability in GPP over CONUS inferred from TROPOMI SIF is larger than what is predicted by either FLUXCOM or FluxSat, both of which show little interannual variability. The low interannual variability is particularly evident in FLUXCOM where we can see small spread in the variability from 2001-2017 (gray lines).

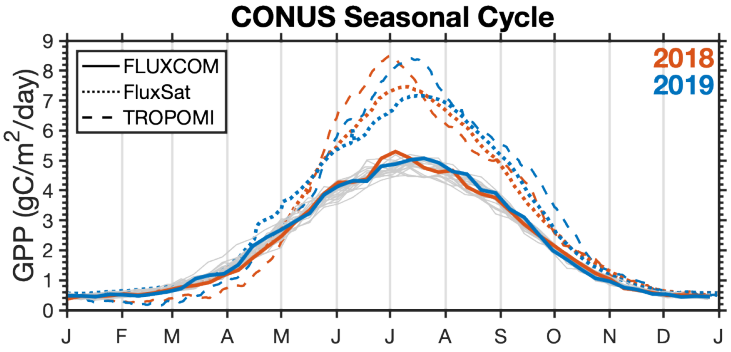


**Figure 5. Comparison of the seasonal cycle inferred from TROPOMI SIF to FLUXCOM and FluxSat.** Red lines indicate the 2018 seasonal cycle and blue lines indicate the 2019 seasonal cycle for TROPOMI (dashed lines), FluxSat (dotted lines), and FLUXCOM (solid lines). Thin gray lines are years 2001–2017 for FLUXCOM.

## 4 Conclusions

We have developed a parsimonious relationship between measurements of SIF from TROPOMI and GPP inferred from flux towers. This relationship allows for estimation of GPP directly from TROPOMI SIF measurements. We combine this SIF-GPP relationship with work downscaling TROPOMI data to 500-m spatial resolution to construct estimates of GPP across the conterminous United States in 2018 and 2019. ~~Our estimate of US GPP varies by less than 4%between 2018 and 2019. We do, however,~~ We observe large regional anomalies that are driven by extreme precipitation events. Namely, west Texas, South Dakota, and California experienced droughts in 2018 while midwestern US crop areas (Illinois, Indiana, and Ohio) experienced flooding in 2019. Taken together, these four events account for 28% of the year-to-year variability in GPP across the conterminous United States. Despite these large regional anomalies, our estimate of US GPP varies by less than 4% between 2018 and 2019.

The impact of the west Texas drought, South Dakota drought, and midwestern flooding are observed in other remote-sensing measures of photosynthetic capacity such as $NIR_V$ while the California drought shows a divergent result using SIF; the divergent responses are driven by specific ecosystems such as evergreen forests. Our work suggests that SIF provides a measure of *photosynthetic activity* as opposed to *photosynthetic capacity*, and converge with other remote-sensing measures under non-stressed conditions. Future work investigating the response to extreme events ~~across ecosystems~~ in evergreen systems may provide additional insight into these divergent responses in remote-sensing measurements related to photosynthesis.

*Acknowledgements.* We are grateful to the team that has realized the TROPOMI instrument, consisting of the partnership between Airbus Defence and Space, KNMI, SRON, and TNO, commissioned by NSO and ESA. We acknowledge the following AmeriFlux sites for their data records: US-ALQ, US-ARM, US-Bi1, US-Bi2, US-CF1, US-CF2, US-CF3, US-CF4, US-CS1, US-CS2, US-CS3, US-EDN, US-GLE, US-Hn2, US-Hn3, US-Ho1, US-JRn, US-Jo2, US-KS3, US-Los, US-Me2, US-Me6, US-Men, US-Mpj, US-MtB, US-Myb, US-NC2, US-NC3,

US-NC4, US-Rls, US-Rms, US-Ro4, US-Ro5, US-Ro6, US-Rwf, US-Rws, US-SRG, US-SRM, US-Seg, US-Ses, US-Sne, US-Snf, US-Syv, US-Ton, US-Tw1, US-Tw4, US-Tw5, US-UMd, US-Var, US-Vcm, US-Vcp, US-WCr, US-Whs, US-Wjs, US-Wkg, US-xAB, US-xBR, US-xCP, US-xDC, US-xDL, US-xHA, US-xJE, US-xJR, US-xKA, US-xKZ, US-xNG, US-xNQ, US-xRM, US-xSE, US-xSL, US-xSP, US-xSR, US-xST, US-xTE, US-xUK, US-xUN, US-xWD, US-xWR, US-xYE. In addition, funding for AmeriFlux data resources was provided by the U.S. Department of Energy's Office of Science. **Funding:** AJT was supported as a Miller Fellow with the Miller Institute for Basic Research in Science at UC Berkeley. This research was funded by grants from the Koret Foundation and NASA 80NSSC19K0945 for support of the computational resources. Part of this research was funded by the NASA Carbon Cycle Science program (grant NNX17AE14G). TROPOMI SIF data generation by PK and CF is funded by the Earth Science U.S. Participating Investigator program (grant NNX15AH95G). TSM was supported through the Macrosystems Biology and NEON-Enabled Science program (DEB-579 1926090). This research used the Savio computational cluster resource provided by the Berkeley Research Computing program at the University of California, Berkeley (supported by the UC Berkeley Chancellor, Vice Chancellor for Research, and Chief Information Officer). **Author contributions:** AJT wrote the text with feedback from all authors. PK and CF performed the TROPOMI SIF retrievals. AJT downscaled the SIF data, conducted the AmeriFlux analysis, and drafted the figures. All authors contributed to the discussion and analysis. **Competing interests:** The authors declare no competing interests. **Data and materials availability:** Daily gridded 500-m TROPOMI SIF and GPP data from February 1, 2018 through June 15, 2020 is temporarily available on Google Drive here: "https://bit.ly/2GHEOOq", and will be uploaded to the ORNL DAAC at acceptance.

## References


Badgley, G., Field, C. B., and Berry, J. A.: Canopy near-infrared reflectance and terrestrial photosynthesis, Sci Adv, 3, e1602 244, https://doi.org/10.1126/sciadv.1602244, 2017.

Badgley, G., Anderegg, L. D. L., Berry, J. A., and Field, C. B.: Terrestrial Gross Primary Production: Using $NIR_V$ to Scale from Site to Globe, Global change biology, https://doi.org/10.1111/gcb.14729, 2019.

Baldocchi, D., Falge, E., Gu, L., Olson, R., Hollinger, D., Running, S., Anthoni, P., Bernhofer, C., Davis, K., Evans, R., Fuentes, J., Goldstein, A., Katul, G., Law, B., Lee, X., Malhi, Y., Meyers, T., Munger, W., Oechel, W., Paw, K. T., Pilegaard, K., Schmid, H. P., Valentini, R., Verma, S., Vesala, T., Wilson, K., and Wofsy, S.: FLUXNET: A New Tool to Study the Temporal and Spatial Variability of Ecosystem–Scale Carbon Dioxide, Water Vapor, and Energy Flux Densities, Bulletin of the American Meteorological Society, 82, 2415–2434, https://doi.org/10.1175/1520-0477(2001)082<2415:fantts>2.3.co;2, 2001.

Baldocchi, D. D., Hicks, B. B., and Meyers, T. P.: Measuring Biosphere-Atmosphere Exchanges of Biologically Related Gases with Micrometeorological Methods, Ecology, 69, 1331–1340, https://doi.org/10.2307/1941631, 1988.

Bishop, C. M.: Pattern Recognition and Machine Learning, Springer, 1 edn., 2007.

Butterfield, Z., Buermann, W., and Keppel-Aleks, G.: Satellite observations reveal seasonal redistribution of northern ecosystem productivity in response to interannual climate variability, Remote Sensing of Environment, 242, 111 755, https://doi.org/10.1016/j.rse.2020.111755, 2020.

Dechant, B., Ryu, Y., Badgley, G., Zeng, Y., Berry, J. A., Zhang, Y., Goulas, Y., Li, Z., Zhang, Q., Kang, M., Li, J., and Moya, I.: Canopy structure explains the relationship between photosynthesis and sun-induced chlorophyll fluorescence in crops, Remote Sensing of Environment, 241, 111 733, https://doi.org/10.1016/j.rse.2020.111733, 2020.

Frankenberg, C., Butz, A., and Toon, G. C.: Disentangling chlorophyll fluorescence from atmospheric scattering effects in $O_2$A-band spectra of reflected sun-light, Geophysical Research Letters, 38, https://doi.org/10.1029/2010gl045896, 2011a.

Frankenberg, C., Fisher, J. B., Worden, J., Badgley, G., Saatchi, S. S., Lee, J.-E., Toon, G. C., Butz, A., Jung, M., Kuze, A., and Yokota, T.: New global observations of the terrestrial carbon cycle from GOSAT: Patterns of plant fluorescence with gross primary productivity, Geophys Res Lett, 38, https://doi.org/10.1029/2011gl048738, 2011b.

Guanter, L., Zhang, Y., Jung, M., Joiner, J., Voigt, M., Berry, J. A., Frankenberg, C., Huete, A. R., Zarco-Tejada, P., Lee, J. E., Moran, M. S., Ponce-Campos, G., Beer, C., Camps-Valls, G., Buchmann, N., Gianelle, D., Klumpp, K., Cescatti, A., Baker, J. M., and Griffis, T. J.: Global and time-resolved monitoring of crop photosynthesis with chlorophyll fluorescence, Proceedings of the National Academy of Sciences of the United States of America, 111, E1327–33, https://doi.org/10.1073/pnas.1320008111, 2014.

He, L., Magney, T., Dutta, D., Yin, Y., Köhler, P., Grossmann, K., Stutz, J., Dold, C., Hatfield, J., Guan, K., Peng, B., and Frankenberg, C.: From the Ground to Space: Using Solar-Induced Chlorophyll Fluorescence to Estimate Crop Productivity, Geophysical Research Letters, 47, https://doi.org/10.1029/2020gl087474, 2020.

Joiner, J. and Yoshida, Y.: Satellite-based reflectances capture large fraction of variability in global gross primary production (GPP) at weekly time scales, Agricultural and Forest Meteorology, 291, 108 092, https://doi.org/10.1016/j.agrformet.2020.108092, 2020.

Jung, M., Schwalm, C., Migliavacca, M., Walther, S., Camps-Valls, G., Koirala, S., Anthoni, P., Besnard, S., Bodesheim, P., Carvalhais, N., Chevallier, F., Gans, F., Goll, D. S., Haverd, V., Köhler, P., Ichii, K., Jain, A. K., Liu, J., Lombardozzi, D., Nabel, J. E. M. S., Nelson, J. A., O'Sullivan, M., Pallandt, M., Papale, D., Peters, W., Pongratz, J., Rödenbeck, C., Sitch, S., Tramontana, G., Walker, A., Weber,

U., and Reichstein, M.: Scaling carbon fluxes from eddy covariance sites to globe: synthesis and evaluation of the FLUXCOM approach, Biogeosciences, 17, 1343–1365, https://doi.org/10.5194/bg-17-1343-2020, 2020.

Köhler, P., Frankenberg, C., Magney, T. S., Guanter, L., Joiner, J., and Landgraf, J.: Global Retrievals of Solar-Induced Chlorophyll Fluorescence With TROPOMI: First Results and Intersensor Comparison to OCO-2, Geophysical Research Letters, 45, 10,456–10,463, https://doi.org/10.1029/2018gl079031, 2018.

Le Quéré, C., Andrew, R. M., Friedlingstein, P., Sitch, S., Hauck, J., Pongratz, J., Pickers, P. A., Korsbakken, J. I., Peters, G. P., Canadell, J. G., Arneth, A., Arora, V. K., Barbero, L., Bastos, A., Bopp, L., Chevallier, F., Chini, L. P., Ciais, P., Doney, S. C., Gkritzalis, T., Goll, D. S., Harris, I., Haverd, V., Hoffman, F. M., Hoppema, M., Houghton, R. A., Hurtt, G., Ilyina, T., Jain, A. K., Johannessen, T., Jones, C. D., Kato, E., Keeling, R. F., Goldewijk, K. K., Landschützer, P., Lefévre, N., Lienert, S., Liu, Z., Lombardozzi, D., Metzl, N., Munro, D. R., Nabel, J. E. M. S., Nakaoka, S.-i., Neill, C., Olsen, A., Ono, T., Patra, P., Peregon, A., Peters, W., Peylin, P., Pfeil, B., Pierrot, D., Poulter, B., Rehder, G., Resplandy, L., Robertson, E., Rocher, M., Rödenbeck, C., Schuster, U., Schwinger, J., Séférian, R., Skjelvan, I., Steinhoff, T., Sutton, A., Tans, P. P., Tian, H., Tilbrook, B., Tubiello, F. N., van der Laan-Luijkx, I. T., van der Werf, G. R., Viovy, N., Walker, A. P., Wiltshire, A. J., Wright, R., Zaehle, S., and Zheng, B.: Global Carbon Budget 2018, Earth System Science Data, 10, 2141–2194, https://doi.org/10.5194/essd-10-2141-2018, 2018.

Lee, J. E., Frankenberg, C., van der Tol, C., Berry, J. A., Guanter, L., Boyce, C. K., Fisher, J. B., Morrow, E., Worden, J. R., Asefi, S., Badgley, G., and Saatchi, S.: Forest productivity and water stress in Amazonia: observations from GOSAT chlorophyll fluorescence, Proc. Biol. Sci., 280, 20130 171, https://doi.org/10.1098/rspb.2013.0171, 2013.

Magney, T. S., Bowling, D. R., Logan, B. A., Grossmann, K., Stutz, J., Blanken, P. D., Burns, S. P., Cheng, R., Garcia, M. A., Köhler, P., Lopez, S., Parazoo, N. C., Raczka, B., Schimel, D., and Frankenberg, C.: Mechanistic evidence for tracking the seasonality of photosynthesis with solar-induced fluorescence, Proceedings of the National Academy of Sciences of the United States of America, 116, 11 640–11 645, https://doi.org/10.1073/pnas.1900278116, 2019.

Magney, T. S., Barnes, M. L., and Yang, X.: On the Covariation of Chlorophyll Fluorescence and Photosynthesis Across Scales, Geophysical Research Letters, 47, https://doi.org/10.1029/2020gl091098, 2020.

Maguire, A. J., Eitel, J. U. H., Griffin, K. L., Magney, T. S., Long, R. A., Vierling, L. A., Schmiege, S. C., Jennewein, J. S., Weygint, W. A., Boelman, N. T., and Bruner, S. G.: On the Functional Relationship Between Fluorescence and Photochemical Yields in Complex Evergreen Needleleaf Canopies, Geophysical Research Letters, 47, https://doi.org/10.1029/2020gl087858, 2020.

Marrs, J. K., Reblin, J. S., Logan, B. A., Allen, D. W., Reinmann, A. B., Bombard, D. M., Tabachnik, D., and Hutyra, L. R.: Solar-Induced Fluorescence Does Not Track Photosynthetic Carbon Assimilation Following Induced Stomatal Closure, Geophysical Research Letters, 47, https://doi.org/10.1029/2020gl087956, 2020.

Monteith, J. L.: Solar Radiation and Productivity in Tropical Ecosystems, Journal of Applied Ecology, 9, 747–766, 1972.

Parazoo, N. C., Bowman, K., Fisher, J. B., Frankenberg, C., Jones, D. B., Cescatti, A., Perez-Priego, O., Wohlfahrt, G., and Montagnani, L.: Terrestrial gross primary production inferred from satellite fluorescence and vegetation models, Global change biology, 20, 3103–21, https://doi.org/10.1111/gcb.12652, 2014.

Reichstein, M., Falge, E., Baldocchi, D., Papale, D., Aubinet, M., Berbigier, P., Bernhofer, C., Buchmann, N., Gilmanov, T., Granier, A., Grunwald, T., Havrankova, K., Ilvesniemi, H., Janous, D., Knohl, A., Laurila, T., Lohila, A., Loustau, D., Matteucci, G., Meyers, T., Miglietta, F., Ourcival, J.-M., Pumpanen, J., Rambal, S., Rotenberg, E., Sanz, M., Tenhunen, J., Seufert, G., Vaccari, F., Vesala, T., Yakir, D., and Valentini, R.: On the separation of net ecosystem exchange into assimilation and ecosystem respiration: review and improved algorithm, Global change biology, 11, 1424–1439, https://doi.org/10.1111/j.1365-2486.2005.001002.x, 2005.

Schaaf, C. B., Gao, F., Strahler, A. H., Lucht, W., Li, X., Tsang, T., Strugnell, N. C., Zhang, X., Jin, Y., Muller, J.-P., Lewis, P., Barnsley, M., Hobson, P., Disney, M., Roberts, G., Dunderdale, M., Doll, C., d'Entremont, R. P., Hu, B., Liang, S., Privette, J. L., and Roy, D.: First operational BRDF, albedo nadir reflectance products from MODIS, Remote Sensing of Environment, 83, 135–148, https://doi.org/10.1016/s0034-4257(02)00091-3, 2002.

Sellers, P. J.: Canopy reflectance, photosynthesis and transpiration, International Journal of Remote Sensing, 6, 1335–1372, https://doi.org/10.1080/01431168508948283, 1985.

Sims, D. A., Brzostek, E. R., Rahman, A. F., Dragoni, D., and Phillips, R. P.: An improved approach for remotely sensing water stress impacts on forest C uptake, Global change biology, 20, 2856–2866, https://doi.org/10.1111/gcb.12537, 2014.

Smith, W. K., Dannenberg, M. P., Yan, D., Herrmann, S., Barnes, M. L., Barron-Gafford, G. A., Biederman, J. A., Ferrenberg, S., Fox, A. M., Hudson, A., Knowles, J. F., MacBean, N., Moore, D. J. P., Nagler, P. L., Reed, S. C., Rutherford, W. A., Scott, R. L., Wang, X., and Yang, J.: Remote sensing of dryland ecosystem structure and function: Progress, challenges, and opportunities, Remote Sensing of Environment, 233, 111 401, https://doi.org/10.1016/j.rse.2019.111401, 2019.

Sun, Y., Fu, R., Dickinson, R., Joiner, J., Frankenberg, C., Gu, L., Xia, Y., and Fernando, N.: Drought onset mechanisms revealed by satellite solar-induced chlorophyll fluorescence: Insights from two contrasting extreme events, Journal of Geophysical Research: Biogeosciences, 120, 2427–2440, https://doi.org/10.1002/2015jg003150, 2015.

Sun, Y., Frankenberg, C., Wood, J. D., Schimel, D. S., Jung, M., Guanter, L., Drewry, D. T., Verma, M., Porcar-Castell, A., Griffis, T. J., Gu, L., Magney, T. S., Kohler, P., Evans, B., and Yuen, K.: OCO-2 advances photosynthesis observation from space via solar-induced chlorophyll fluorescence, Science, 358, https://doi.org/10.1126/science.aam5747, 2017.

Sun, Y., Frankenberg, C., Jung, M., Joiner, J., Guanter, L., Köhler, P., and Magney, T.: Overview of Solar-Induced chlorophyll Fluorescence (SIF) from the Orbiting Carbon Observatory-2: Retrieval, cross-mission comparison, and global monitoring for GPP, Remote Sensing of Environment, 209, 808–823, https://doi.org/10.1016/j.rse.2018.02.016, 2018.

Turner, A. J. and Jacob, D. J.: Balancing aggregation and smoothing errors in inverse models, Atmos Chem Phys, 15, 7039–7048, https://doi.org/10.5194/acp-15-7039-2015, 2015.

Turner, A. J., Köhler, P., Magney, T. S., Frankenberg, C., Fung, I., and Cohen, R. C.: A double peak in the seasonality of California's photosynthesis as observed from space, Biogeosciences, 17, 405–422, https://doi.org/10.5194/bg-17-405-2020, 2020.

USDA: National Agricultural Statistics Service Cropland Data Layer: Published crop-specific data layer, https://nassgeodata.gmu.edu/CropScape/, 2018.

Veefkind, J. P., Aben, I., McMullan, K., Förster, H., de Vries, J., Otter, G., Claas, J., Eskes, H. J., de Haan, J. F., Kleipool, Q., van Weele, M., Hasekamp, O., Hoogeveen, R., Landgraf, J., Snel, R., Tol, P., Ingmann, P., Voors, R., Kruizinga, B., Vink, R., Visser, H., and Levelt, P. F.: TROPOMI on the ESA Sentinel-5 Precursor: A GMES mission for global observations of the atmospheric composition for climate, air quality and ozone layer applications, Proc SPIE, 120, 70–83, https://doi.org/10.1016/j.rse.2011.09.027, 2012.

Wang, X., Dannenberg, M. P., Yan, D., Jones, M. O., Kimball, J. S., Moore, D. J. P., Leeuwen, W. J. D., Didan, K., and Smith, W. K.: Globally Consistent Patterns of Asynchrony in Vegetation Phenology Derived From Optical, Microwave, and Fluorescence Satellite Data, Journal of Geophysical Research: Biogeosciences, 125, https://doi.org/10.1029/2020jg005732, 2020.

Yang, H., Yang, X., Zhang, Y., Heskel, M. A., Lu, X., Munger, J. W., Sun, S., and Tang, J.: Chlorophyll fluorescence tracks seasonal variations of photosynthesis from leaf to canopy in a temperate forest, Global change biology, 23, 2874–2886, https://doi.org/10.1111/gcb.13590, 2017.

Yang, X., Tang, J., Mustard, J. F., Lee, J.-E., Rossini, M., Joiner, J., Munger, J. W., Kornfeld, A., and Richardson, A. D.: Solar-induced chlorophyll fluorescence that correlates with canopy photosynthesis on diurnal and seasonal scales in a temperate deciduous forest, Geophysical Research Letters, 42, 2977–2987, https://doi.org/10.1002/2015gl063201, 2015.

Yao, J., Liu, H., Huang, J., Gao, Z., Wang, G., Li, D., Yu, H., and Chen, X.: Accelerated dryland expansion regulates future variability in dryland gross primary production, Nature communications, 11, https://doi.org/10.1038/s41467-020-15515-2, 2020.

Yin, Y., Byrne, B., Liu, J., Wennberg, P. O., Davis, K. J., Magney, T., Köhler, P., He, L., Jeyaram, R., Humphrey, V., Gerken, T., Feng, S., Digangi, J. P., and Frankenberg, C.: Cropland Carbon Uptake Delayed and Reduced by 2019 Midwest Floods, AGU Advances, 1, https://doi.org/10.1029/2019av000140, 2020.